Effectiveness of Loop Anchorages for Reinforcement in Precast Concrete Members

Alan H. Mattock
Ph.D., S.E.
Professor Emeritus of
Civil Engineering
University of Washington
Seattle, Washington

Loop anchorages are an effective means of providing anchorage for tie reinforcement when detailing discontinuity regions in reinforced or prestressed, precast concrete members using strut and tie models. However, the ACI Building Code does not contain guidance on the use of loop anchorages. An experimental study on the effectiveness of loop anchorages when subject to various levels of compression across the plane containing the loop is described in this paper. Based on the data obtained, design proposals are made for 180-degree loops in Nos. 4, 5, and 6 reinforcing bars with the minimum bend diameter allowed by the ACI Code. Numerical design examples illustrate the proposed design method.

When using the strut and tie method to detail discontinuity regions in structural concrete members, it is frequently necessary to provide positive anchorages for ties at nodes in the truss model. A 180-degree loop in the reinforcing bar used for the tie is one possibility.[1] An example of this is the use of a loop to anchor the hanger reinforcement in a dapped end.

The effectiveness of such a loop anchorage was demonstrated by Mattock and Theryo,[2] who tested precast, prestressed T-beams containing this type of hanger reinforcement with both vertical and sloping end face dapped ends. The yield strength of the hanger

reinforcement was developed for both configurations; however, it was not possible to determine how much of the force in the hanger reinforcement was resisted by the loop and how much was resisted by the straight parts of the bars leading into the loop.

Fig. 1 from Ref. 2 shows the cracking pattern after failure of a sloping end face dapped end, in which the hanger reinforcement was anchored by a loop at its upper end. The loop had a bend diameter of six bar diameters and concrete cover of $^3/_4$ in. (19 mm). The cracking pattern indicates that strutting action occurred within the nib of the dapped end, between the flexural compression zone above the re-entrant
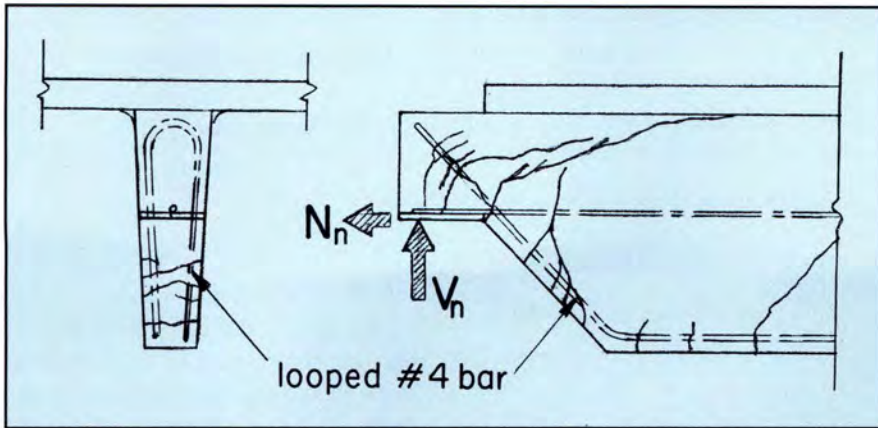
Fig. 1. Cracking pattern after failure of a dapped end with hanger reinforcement anchored by a 180-degree loop (Ref. 2).

Fig. 2. Typical test specimen.

corner and the anchor zone of the hanger reinforcement, and between the support and the anchor zone of the hanger reinforcement.

It is the presence of the compression forces acting across the plane of the loop anchorage that restrains splitting of the concrete in that plane, and so enables the loop anchorage to resist the tension forces in the hanger reinforcement. Yield of the hanger reinforcement initiated close to the re-entrant corner and spread along the reinforcement in the nib, as evidenced by splitting cracks along the hanger reinforcement. At failure, the hanger reinforcement must have been yielding close to the anchorage loop.

The extent of yielding in the hanger reinforcement of the dapped end beams tested indicated that a loop of minimum bend diameter can be a more efficient anchorage than the ACI Code[3] standard hook, which requires a significant lead-in length of straight bar if the yield strength of the bar is to be developed. This is probably because failures corresponding to those caused by opening up of a hook are eliminated in the case of the loop anchorage.

The ACI Code[3] does not contain any guidance on the design of loop anchorages. Section 17.4.1.3 of the CEB-FIP Model Code[4] requires that, for loop anchorages, "A calculation check should be made for splitting of the concrete in the plane of a loop anchorage." An accompanying "Note" says that, "It can be assumed that splitting will not occur if the diameter D of the mandrel used in making the loop is such that:

$$D \geq \left[\left(0.7 + 1.4 \frac{d_b}{z} \right) \frac{f_s}{1.5 f_{cd}} \right] d_b \quad (17.8)$$

where f_s is the stress in the bar at the start of the bend and z is the smaller of the two following quantities:
• distance between the centers of two adjacent loops
• the cover c increased by half the bar diameter d_b."

In the above equation, f_{cd} is the design concrete strength, which is the characteristic strength f_{ck} divided by the material strength reduction factor $\gamma_c = 1.5$. Also, the CEB Model Code[4] states that f_{ck} may be taken as the
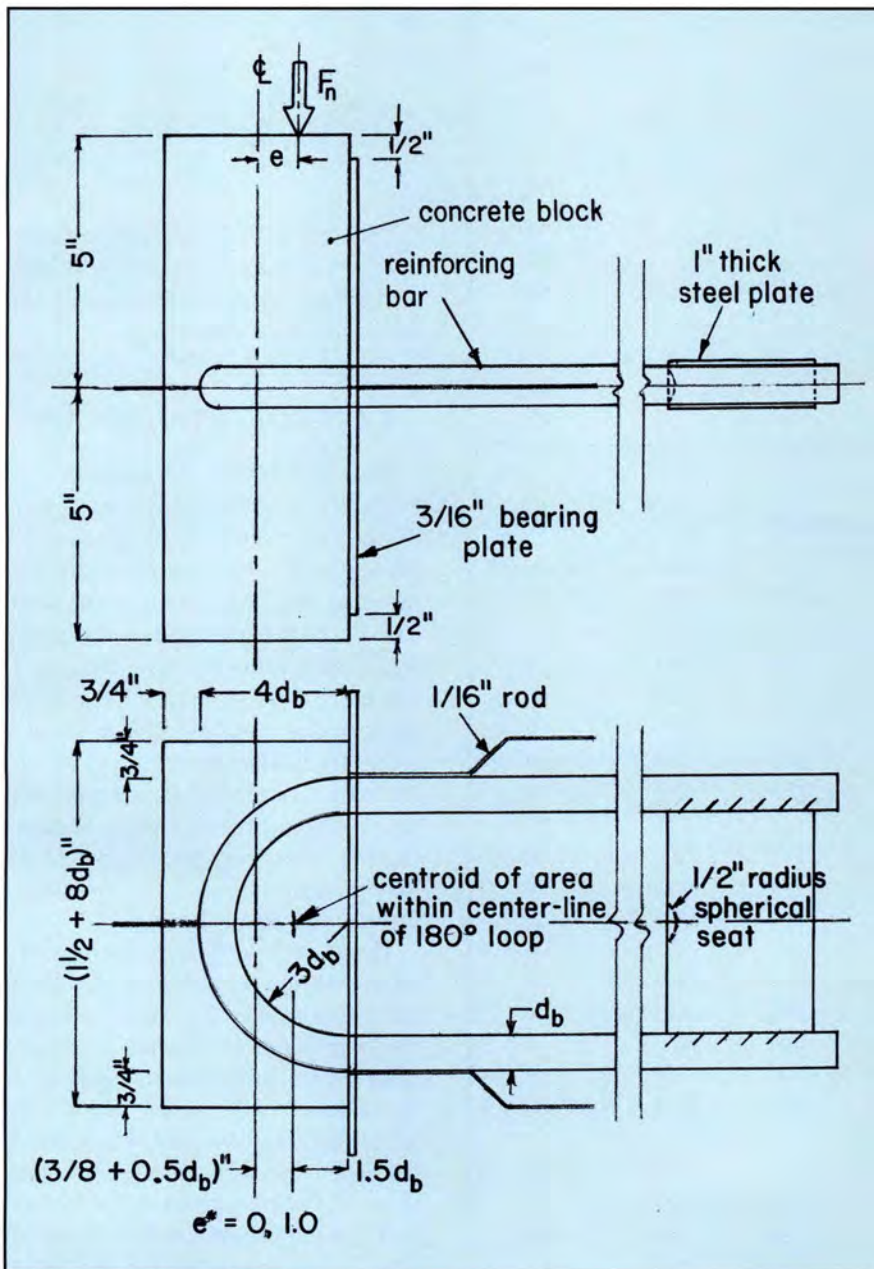
Table 1. Series A — Specimens with zero lateral force.

Specimen number	f_c' (psi)	f_{ct} (psi)	Specimen number	f_c' (psi)	f_{ct} (psi)
4-0-3210	3210	355	4-0-4840	4840	455
5-0-3210	3210	355	5-0-4840	4840	455
6-0-3210	3210	355	6-0-4840	4840	455
4-0-3450	3450	360	5-0-6110	6110	550
5-0-3450	3450	360	6-0-6110	6110	550
6-0-3450	3450	360	5-0-6450	6450	565
			6-0-6450	6450	565

Note: 1000 psi = 6.895 MPa.

Table 2. Series B — Specimens with concentric lateral force ($e = 0$).

Specimen number	f_c' (psi)	f_{ct} (psi)	Lateral force (kips)	f_n (psi)
4-75-3410-0	3410	370	1.13	75
5-75-3410-0	3410	370	1.58	75
6-75-3410-0	3410	370	2.11	75
4-175-2920-0	2920	330	2.65	175
5-175-2920-0	2920	330	3.70	175
6-175-2920-0	2920	330	4.92	175
4-350-3620-0	3620	375	5.29	350
5-350-3620-0	3620	375	7.39	350
6-350-3420-0	3420	355	9.84	350
5-400-3700-0	3700	415	8.45	400
4-500-3300-0	3300	350	7.56	500
5-500-3300-0	3300	350	10.56	500
6-500-3300-0	3300	350	14.06	500
4-615-3480-0	3480	400	9.30	615
5-615-3480-0	3480	400	12.99	615
6-615-3480-0	3480	400	17.30	615

Note: 1000 psi = 6.895 MPa; 1 kip = 4.46 kN.

Table 3. Series C — Specimens with eccentric lateral force ($e \neq 0$).

Specimen number	f_c' (psi)	f_{ct} (psi)	Lateral force (kips)	f_n (psi)	Eccentricity e (in.)	Eccentricity $e*$
$e* = 1.0$						
4-75-3460-1	3460	390	1.13	75	0.63	1.0
5-75-3460-1	3460	390	1.58	75	0.69	1.0
6-75-3460-1	3460	390	2.11	75	0.75	1.0
4-225-3960-1	3960	410	3.4	225	0.63	1.0
5-225-3960-1	3960	410	4.75	225	0.69	1.0
6-225-3960-1	3960	410	6.33	225	0.75	1.0
5-350-3430-1	3430	370	7.39	350	0.69	1.0
6-350-3420-1	3420	355	9.84	350	0.75	1.0
5-400-3700-1	3700	415	8.45	400	0.69	1.0
4-500-3530-1	3530	380	7.56	500	0.63	1.0
5-500-3530-1	3530	380	10.56	500	0.69	1.0
6-500-3530-1	3530	380	14.06	500	0.75	1.0
4-600-3680-1	3680	365	9.08	600	0.63	1.0
5-600-3680-1	3680	365	12.68	600	0.69	1.0
6-600-3680-1	3680	365	16.88	600	0.75	1.0
$e* \neq 1$ or 0						
5-350-3420-0.5	3420	355	7.39	350	0.31	0.5
5-400-3700-1.5	3700	415	8.45	400	1.03	1.5
5-350-3430-1.75	3430	370	7.39	350	1.20	1.75
5-350-3430-(-1)	3430	370	7.39	350	-0.69	-1.0

Note: 1000 psi = 6.895 MPa; 1 kip = 4.46 kN; 1 in. = 25.4 mm.

mean cylinder strength f_{cm} less 8 MPa, i.e., $(f_c' - 1.16 \text{ ksi})$ if f_c' is the average compressive strength in ksi.

Using customary units, Eq. (17.8) for a single loop may be restated as:

Minimum bend diameter:

$$D = \left[\left\{ 0.7 + \left(\frac{1.4 d_b}{c + 0.5 d_b} \right) \right\} \frac{f_s}{\left(f_c' - 1.16 \right)} \right] d_b$$

(1a)

Using SI units, Eq. (1a) becomes:

Minimum bend diameter:

$$D = \left[\left\{ 0.7 + \left(\frac{1.4 d_b}{c + 0.5 d_b} \right) \right\} \frac{f_s}{\left(f_c' - 8 \right)} \right] d_b$$

(1b)

If D = ACI Code minimum = $6d_b$ for bar sizes 3 through 8, then Eq. (1) may be transposed to yield the bar stress at the point of tangency of the loop:

$$f_s = 6 \left(f_c' - 1.16 \right) \left[\frac{c + 0.5 d_b}{0.7c + 1.75 d_b} \right] \text{ksi}$$

(2a)

or

$$f_s = 6 \left(f_c' - 8 \right) \left[\frac{c + 0.5 d_b}{0.7c + 1.75 d_b} \right] \text{MPa}$$

(2b)

The CEB-FIP Model Code[4] equation does not take into account the beneficial effect of lateral compression across the plane of the loop.

EXPERIMENTAL STUDY

The objective of this study was to evaluate the effectiveness of a 180-degree loop anchorage of $6d_b$ bend diameter with $3/4$ in. (19 mm) cover at the sides and at the head of the loop. The variables included in the study were: reinforcing bar size, Nos. 4, 5, and 6 (12.7, 15.9, and 19.1 mm in diameter); compressive strength of concrete, from 3000 to 6450 psi (21 to 44 MPa); intensity of compressive stress acting across the plane containing the loop, zero to 615 psi (4.24 MPa); and eccentricity of the lateral force acting across the loop.

Three series of specimens were tested: Series A, in which no lateral force was applied across the plane of the loop; Series B, in which a uniform compressive stress was applied across the plane of the loop; and Series C, in which an eccentric load was applied, causing a varying compressive stress across the plane containing the loop.

A typical test specimen is shown in Fig. 2. The dimensions of the specimens varied with the size of reinforc-

ing bar, as shown in the figure. The $^1/_{16}$ in. (1.6 mm) diameter steel rods were silver soldered to the reinforcing bar for use in measuring slip of the reinforcing bar at the head of the loop and at the bearing face during the test.

Materials and Fabrication

The concrete was made from Type 3 portland cement, $^7/_8$ in. (22 mm) maximum size glacial outwash gravel, sand, and water. The Nos. 4, 5, and 6 deformed reinforcing bars conformed to ASTM Standard 706 and had yield strengths of 66.0, 71.9, and 61.9 ksi (455, 496, and 427 MPa) respectively, based on nominal bar areas. All the bars had a clearly defined yield point.

The reinforcing bars were cold bent to form 180-degree loops with a bend diameter of $6d_b$ and with the longitudinal ribs of the bars in the plane of the loop. Each looped bar was inserted through two holes in a $^3/_{16}$ in. (4.8 mm) thick steel plate, which formed part of the formwork for the concrete block and was later used as a bearing plate during the test. A 1 in. (25.4 mm) thick piece of steel plate with a $^1/_2$ in. (12.7 mm) radius spherical depression ground in one edge, was welded between the ends of the reinforcing bar. The center of the spherical depression was located in the plane containing the centerline of the loop and midway between the straight portions of the reinforcing bar. The $^1/_{16}$ in. (1.6 mm) wires used for slip measurement were then attached to the reinforcing bar.

The form for each size of specimen was mounted on a plywood base, to which was also attached a jig to locate the reinforcing bar accurately at mid-height of the form and normal to the bearing face. The front face of the form was formed by the $^3/_{16}$ in. (4.8 mm) steel plate through which the reinforcing bar loop was threaded, together with additional $^1/_2$ in. (12.7 mm) wide strips of $^3/_{16}$ in. (4.8 mm) plate at top and bottom. (These strips were provided so that the bearing plate would not interfere with the application of vertical load to the specimen during the test.) The small gaps around the reinforcing bar where it passed through the $^3/_{16}$ in. (4.8 mm) plate were filled with putty. The back
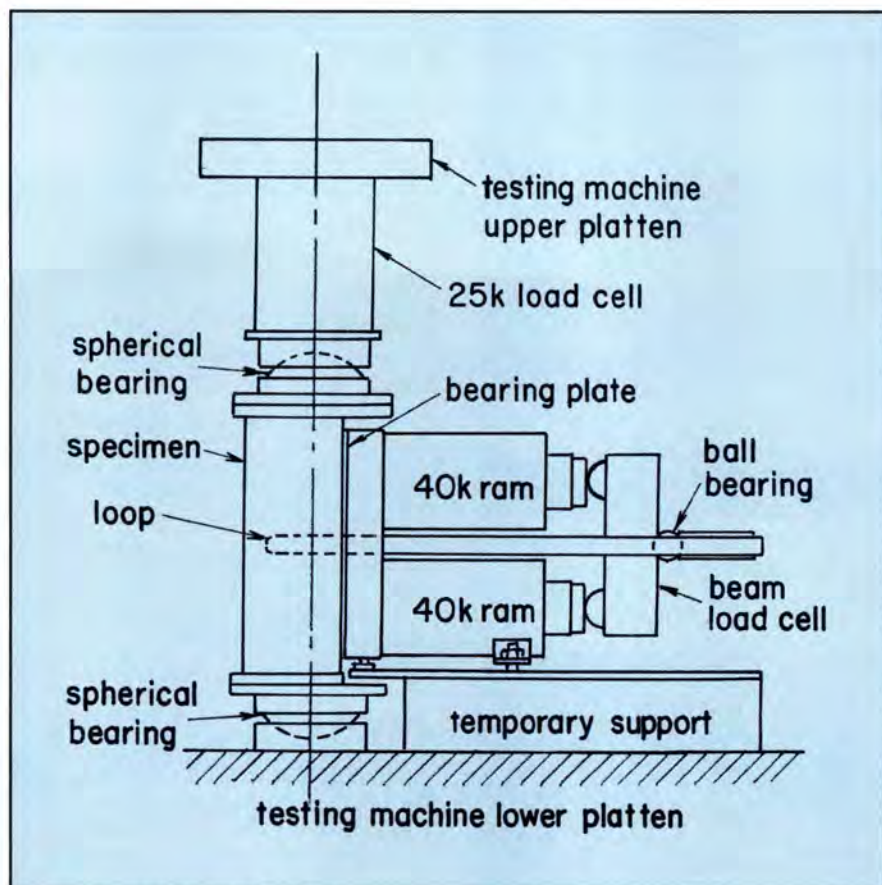

Fig. 3. Arrangements for test.

and sides of the form were of $^3/_4$ in. (19 mm) coated plywood.

The specimens were, in general, cast in sets of three, one of each bar size. The specimens and accompanying 6 x 12 in. (150 x 300 mm) cylinders were covered with polyethylene sheets for 24 hours. At that time they were removed from the forms and cured in air until test at age 3 days. The specimens and the cylinders were capped on both top and bottom faces with high strength gypsum plaster.

The compressive and splitting tensile strengths of the concrete in the specimens at time of test are listed in Tables 1, 2 and 3. The numbering of the specimens is of the form A – B – C – D, where A is the bar size, B is the average compressive stress f_n acting across the plane of the loop in psi, C is the compressive strength of the concrete in psi, and D is the non-dimensional eccentricity e^*.

When the eccentricity e of the lateral force with respect to the centroid of the cross section of the specimen in Series B and C and the bar diameter d_b are measured in inches:

$$e^* = e/(0.5d_b + 0.375) \qquad (3a)$$

When e and d_b are measured in millimeters:

$$e^* = e/(0.5d_b + 9.53) \qquad (3b)$$

Testing Arrangements and Test Procedures

The testing arrangements for the specimens of Series A and B are shown in Fig. 3. The lateral force F_n was provided by a 300 kip (1334 kN) capacity Baldwin hydraulic testing machine. This force was applied through a 25 kip (111 kN) capacity load cell and a 2.5 in. (50 mm) radius spherical bearing. The specimen was supported on the lower platten of the testing machine on a similar spherical bearing so that the line of action of the lateral force could be accurately located. The spherical bearings were arranged so that their centers of rotation were at the top and bottom faces of the test specimen. Two 4-mil sheets of Teflon were placed between the faces of the spherical bearings to minimize friction.
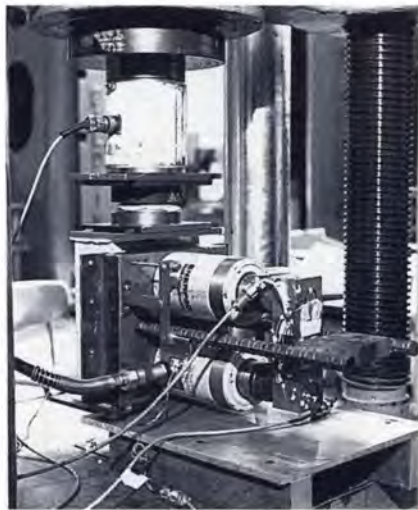
Fig. 4. Test in progress showing the loading side of the test arrangement.
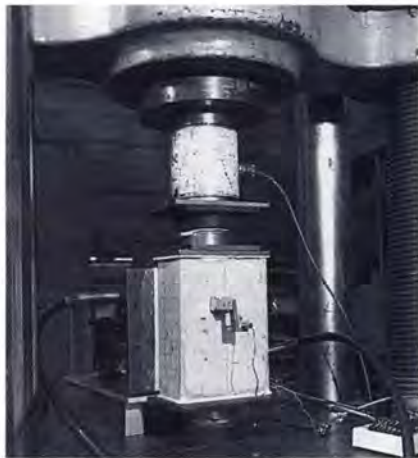

Fig. 5. Test in progress showing the rear of the test specimen.

The tensile force P was applied symmetrically to the two legs of the loop by two 40 kip (178 kN) hydraulic rams acting through a beam type load cell and a 1 in. (25.4 mm) diameter ball bearing. The hydraulic rams were mounted on the 1.5 in. (38 mm) thick steel plate through which the reinforcing bars passed. The back of this plate rested against the $^3/_{16}$ in. (4.8 mm) bearing plate. Sandwiched between this plate and the bearing face of the concrete specimen were two sheets of 4-mil Teflon, to reduce friction between the bearing plate and the specimen and so minimize any restraint to splitting of the specimen by such friction. (The coefficient of friction with this arrangement was found to be approximately 0.012.)

Before the test, the hydraulic ram assembly was clamped to the test speci-

men with large C-clamps. The whole assembly was then temporarily supported by a platform resting on the lower platten of the testing machine, as seen in Fig. 3. The C-clamps were removed and the supporting screws between the lower ram and the supporting platform were retracted in the test, when the pull-out load reached 1 kip (4.5 kN).

In the case of Series A, where no lateral force F_n was applied, the ar-

rangements for applying the pull-out force were the same. However, in this case the ram assembly was supported on the platform during the test and the top and bottom faces of the specimen were free.

The movement (slip) of the reinforcement at the bearing face and at the head of the loop was measured by Linear Variable Deferential Transformers (LVDTs), whose cores were

Table 4. Test results for Series A — Specimens with zero lateral force.

Specimen number	Load at first crack (kips)	HL slip* at maximum load (in.)	BF slip† at maximum load (in.)	Failure load, P_f (kips)	$P_{f\,calc}$ ‡ (kips)	$\dfrac{P_{f\,test}}{P_{f\,calc}}$	Failure type§
4-0-3210	1.39	0.004	0.020	5.06	4.78	1.06	SF
5-0-3210	2.71	0.004	0.024	8.30	6.68	1.24	SF
6-0-3210	6.81	0.006	0.028	13.90	8.89	1.56	SF
4-0-3450	1.77	0.012	0.036	5.15	4.85	1.06	SF
5-0-3450	2.25	0.006	0.048	4.58	6.77	0.68	SF
6-0-3450	3.20	0.011	0.054	11.01	9.01	1.22	SF
4-0-4840	1.55	0.010	0.032	6.35	6.13	1.04	SF
5-0-4840	1.71	0.007	0.041	6.78	8.56	0.79	SF
6-0-4840	2.69	0.004	0.037	11.01	9.01	1.22	SF
5-0-6110	2.14	0.005	0.039	9.24	10.34	0.89	SF
6-0-6110	3.99	0.006	0.043	15.99	13.77	1.16	SF
5-0-6450	2.30	0.003	0.033	9.90	10.62	0.93	SF
6-0-6450	2.60	0.006	0.042	11.70	14.15	0.83	SF

Note: 1 in. = 25.4 mm; 1 kip = 4.46 kN.
* Slip of head of loop.
† Slip of bearing face of specimen.
‡ $P_f = 0.89 f_{ct} A$.
§ SF = splitting failure.

Table 5. Test results for Series B — Specimens with concentric lateral force.

Specimen number	Load at first crack (kips)	HL slip* at maximum load (in.)	BF slip† at maximum load (in.)	Failure load, P_f (kips)	$P_{f\,calc}$ ‡ (kips)	$\dfrac{P_{f\,test}}{P_{f\,calc}}$	Failure type§
4-75-3410-0	2.83	0.004	0.028	10.14	9.56	1.06	SF
5-75-3410-0	2.46	0.014	0.057	11.11	13.36	0.83	SF
6-75-3410-0	3.90	0.009	0.057	16.48	17.81	0.93	SF
4-175-2920-0	4.57	0.017	0.052	14.96	12.49	1.20	SF
5-175-2920-0	3.39	0.021	0.085	18.62	17.44	1.07	SF
6-175-2920-0	6.89	0.016	0.070	28.11	23.20	1.21	SF
4-350-3620-0	3.81	0.016	0.060	16.37	18.61	0.88	SF
5-350-3620-0	7.12	0.019	0.059	27.30	25.99	1.05	SF
6-350-3420-0	8.80	0.020	0.083	34.62	33.69	1.03	SF
5-400-3700-0	9.96	0.025	0.079	29.07	29.25	0.99	SF
4-500-3300-0	2.84	0.041	0.066	22.80	21.76	1.05	SF
5-500-3300-0	7.76	0.032	0.102	32.05	30.40	1.05	SF
6-500-3300-0	7.13	0.053	0.126	38.53	40.47	0.95	SF
4-615-3480-0	5.02	0.053	0.133	22.14	25.90	0.86	SF
5-615-3480-0	8.07	0.035	0.083	32.29	36.18	0.89	SF
6-615-3480-0	14.11	0.037	0.092	48.39	48.18	1.00	SF

Note: 1 in. = 25.4 mm; 1 kip = 4.46 kN.
* Slip of head of loop.
† Slip of bearing face of specimen.
‡ $P_f = f_{ct} A [0.89 + 2.51(f_n/f_{ct})^{0.70}]$.
§ SF = splitting failure.

connected through brass extensions to the $^1/_{16}$ in. (1.6 mm) rods attached to the reinforcing bar, as shown in Fig. 2. The bodies of the LVDTs were supported by brass fittings mounted on the 1.5 in. (38 mm) thick bearing plate and on the rear face of the specimen, as seen in Figs. 4 and 5. These LVDTs and the beam load cell used to measure the pull-out force were connected to a Vishay-Ellis automatic data logging system. The 25 kip (111 kN) capacity load cell was connected to a Budd strain gauge indicator.

In test Series B and C, the lateral force F_n was first applied by the Baldwin testing machine. When the required load was reached, the Budd indicator connected to the 25 kip (111 kN) load cell was balanced at zero. The lateral force was maintained at a constant during the test by keeping the Budd indicator on zero, through adjustment of the testing machine controls.

The pull-out load P was increased incrementally. So as to complete the test in approximately 30 minutes, the increments were typically varied as follows:

1. 0.5 kip (2.2 kN) increments until the first crack was observed in the specimen.

2. One to 2 kip (4.5 and 9 kN) increments until failure appeared imminent.

3. 0.5 kip (2.2 kN) increments until failure, which was considered to have occurred when the pull-out load could not be increased further, nor be maintained.

At each increment, measurements of pull-out load and slip were made and any new cracks were marked on the visible faces of the specimen. After failure, the pull-out load was reduced as slowly as possible and additional measurements of slip were made.

Specimen Strength and Behavior

The test results are summarized in Tables 4, 5, and 6, for Series A, B, and C, respectively. These include the pull-out load at first cracking and at failure, the movement of the head of the loop (HL Slip) and the average slip of the reinforcing bar at the bearing face of the specimen (BF Slip), at

Table 6. Test results for Series C — Specimens with eccentric lateral force.

Specimen number	Load at first crack (kips)	HL slip* at maximum load (in.)	BF slip† at maximum load (in.)	Failure load, P_f (kips)	$P_{f\,calc}$ ‡ (kips)	$\dfrac{P_{f\,test}}{P_{f\,calc}}$	Failure type§
$e* = 1.0$							
4-75-3460-1	3.23	0.001	0.022	9.42	10.26	0.92	SF
5-75-3460-1	3.34	0.000	0.012	14.60	14.33	1.02	SF
6-75-3460-1	5.26	–	0.034	20.18	19.08	1.06	SF
4-225-3960-1	3.34	0.001	0.010	17.53	17.57	1.00	SF
5-225-3960-1	5.07	0.009	0.031	24.14	24.54	0.98	SF
6-225-3960-1	11.72	0.002	0.012	34.26	32.67	1.05	SF
5-350-3430-1	7.49	0.003	0.028	33.20	31.19	1.06	SF
6-350-3420-1	17.75	0.001	0.020	42.55	41.00	1.04	SF
5-400-3700-1	8.93	0.005	0.020	34.78	35.47	0.98	SF
4-500-3530-1	20.68	0.010	0.043	30.86	29.19	1.06	BYSF
5-500-3530-1	6.73	0.003	0.015	37.18	40.76	0.91	SF
6-500-3530-1	11.72	0.003	0.023	51.50	54.27	0.95	SF
4-600-3680-1	9.89	0.005	0.019	34.79	33.49	1.04	BY
5-600-3680-1	9.90	0.003	0.017	48.29	46.78	1.03	BYSF
6-600-3680-1	19.88	0.004	0.022	59.8	62.27	0.96	BY
$e* \neq 0$ or 1							
5-350-3420-0.5	3.94	0.001	0.012	26.90	28.05	0.96	SF
5-400-3700-1.5	6.21	0.005	0.020	37.26	38.58	0.97	SF
5-350-3430-1.75	9.51	0.004	0.032	35.24	35.22	1.00	SF
5-350-3430-(-1)	9.99	0.001	0.017	18.30	20.45	0.89	SF

Note: 1 in. = 25.4 mm; 1 kip = 4.46 kN.
* Slip of head of loop.
† Slip of bearing face of specimen.
‡ $P_f = f_{ct}A[0.89 + 2.51(f_n/f_{ct})^{0.70} + 0.75e*(f_n/f_{ct})^{1.55}]$.
§ SF = splitting failure; BY = rebar yielded; BYSF = splitting failure after yield of rebar.

maximum load. Also shown is the type of failure of each specimen.

In Series A, where no lateral force was applied to the specimen, the pull-

out load at first cracking averaged 30 percent of the failure load with a standard deviation of 9 percent. The ratio of the two loads tended to decrease
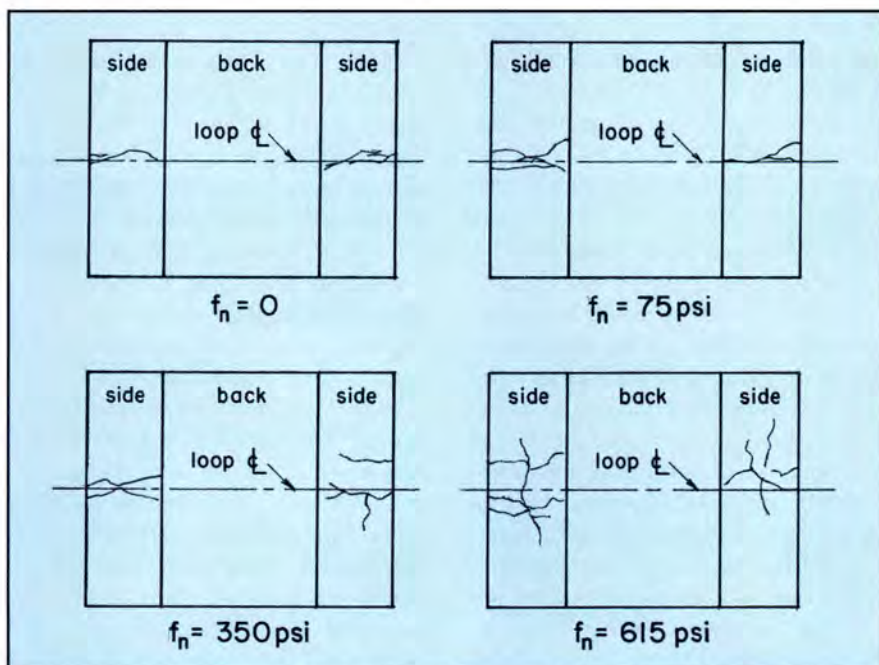

Fig. 6. Typical variation of cracking pattern with level of concentric lateral force ($f_n = F_n/A$).

as the concrete strength increased, ranging from 0.36 for an f_c' of 3200 psi (22 MPa) to 0.23 for an f_c' of 6000 psi (42 MPa).

In Series B, where the specimens were subject to a concentric lateral force that created a uniform compressive stress, the pull-out load at first cracking averaged 24 percent of the failure load, with a standard deviation of 5 percent. In this case, the ratio of the two loads did not vary with the concrete strength, or with either intensity of lateral force f_n or bar diameter.

The ratio was more consistent when a uniform compressive stress was acting across the plane of the reinforcement loop than when no compressive stress was acting. This was possibly due to the reduced significance of random variation of the tensile strength of the concrete when a uniform compressive stress acts across the plane of the loop; also, the effect of any slight misalignment of the reinforcing bar in the specimen would be reduced when compression acts across the plane of the loop.

In Series C, where an eccentric lateral force was applied to the specimen creating a varying compressive stress in the specimen, the pull-out load at first cracking averaged 29 percent of the failure load, with a standard deviation of 12 percent. In this series, the eccentric lateral force creates a tensile stress at the back face of the specimen that varies with both the eccentricity of the lateral force and the size of the specimen. This may be responsible for the greater scatter in the value of the ratio of the cracking load to the failure load.

Fig. 6 shows typical patterns of cracking just before failure for a group of specimens with approximately constant concrete strength, but each specimen being subject to a different concentric lateral force, i.e., uniform stress f_n in the plane of the loop. It can be seen that the cracking becomes more extensive as f_n increases. Also, at higher levels of lateral stress f_n, vertical cracks occur in addition to the horizontal cracks in the vicinity of the reinforcing bar loop. In general, the cracking initiated at the bearing face, approximately in the plane of the reinforcing bar loop, and propagated to-
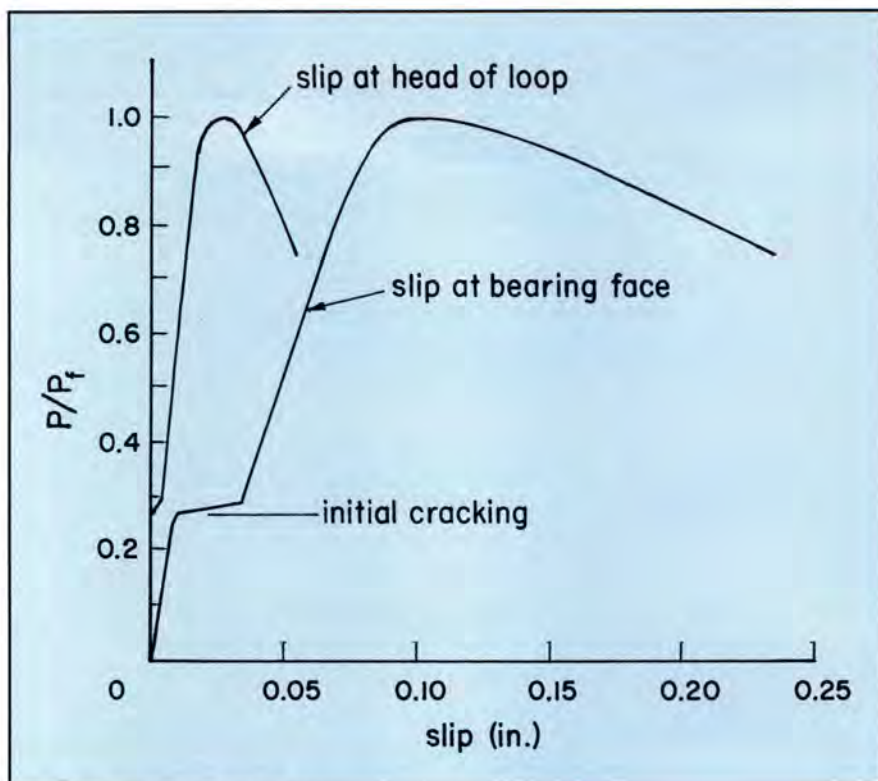

Fig. 7. Typical load-slip curves.

ward the back face of the specimen as the pull-out load increased. The initiation of cracking at the bearing face of the specimen is consistent with the occurrence there of the highest bond stresses between the reinforcing bar and the concrete.

In the cases where vertical cracks occurred, these cracks initiated at the horizontal cracks, approximately halfway toward the back face of the specimen. When specimens were taken apart after testing, it was seen that in the interior of the specimen the vertical cracks essentially followed the centerline of the reinforcing bar loop. These cracks were probably caused by a combination of the Poisson effect due to the lateral force F_n and the bearing force exerted by the reinforcing bar loop on its inside face.

Fig. 7 shows typical load–slip curves. The load P is expressed as a proportion of the pull-out load at failure, P_f. The curves for individual specimens showed some variability, but the general shape of the curves was that shown in Fig. 7. The curve of slip measured at the bearing face was quite steep until the initial cracking load was reached, corresponding to the development of adhesion bond between

the reinforcing bar and the concrete. After cracking initiated, the adhesion bond was destroyed and subsequent bond forces were transferred primarily by bearing of the reinforcing bar lugs on the concrete. The pull-out force was resisted by a combination of these bond forces and by bearing between the inside of the reinforcing bar loop and the concrete.

The slip at the bearing face usually increased suddenly at cracking, as the cracks spread toward the rear of the specimen. When the cracking stabilized, the slope of the slip curve became steeper as the reinforcing bar lugs engaged the concrete. As failure was approached, the slope of the bearing face slip curve gradually decreased to zero at maximum load. The downward slope of this curve after maximum load was steepest when no lateral force was acting, in which case failure was quite brittle. The slope of the curve became flatter as the magnitude of the lateral force increased.

Until cracking initiated adjacent to the bearing face, no movement of the head of the loop occurred. The slope of the curve of slip at the head of the loop was much steeper than the curve of bearing face slip. At lower levels of

lateral force, the head of the loop tended to move in more rapidly as the cracking propagated toward the rear face. At higher levels of lateral force, the cracks propagated more slowly and this initially "soft" behavior did not occur. The slip at maximum load at the head of the loop was approximately one quarter of that at the bearing face.

When the specimens were taken apart after testing, a wedge shaped piece of concrete was often found sticking to the inner face of the reinforcing bar loop.

Discussion of Test Results

Series A, zero lateral force — It appeared reasonable to expect that in this case, the pull-out strength of the loop would depend on the tensile strength of the concrete in the plane of the loop because the failure mode in all the tests was splitting of the specimen in the plane containing the loop. The pull-out force P_f was, therefore, plotted against the product of the measured splitting tensile strength of the concrete, f_{ct}, and the cross-sectional area of the specimen in the plane of the loop, A (see Fig. 8). Although the splitting tensile strength of the concrete is not equal to its direct tensile strength, it serves as a measure of the tensile strength in the same way that the compressive strength of the 6 x 12 in. (150 x 300 mm) cylinder serves as a measure of the true compressive strength of the concrete. It can be seen that the variation of P_f with $f_{ct}A$ can reasonably be represented by the straight line corresponding to:

$$P_f = 0.89 f_{ct} A \qquad (4)$$

The values of P_f calculated using Eq. (4) are listed in Table 4. The average value of the ratio $P_f(\text{test})/P_f(\text{calc.})$ for Series A is 1.02, with a standard deviation of 0.242. The scatter of the test results does not appear to be related to the reinforcing bar diameter. This variable is apparently accounted for satisfactorily by the inclusion in Eq. (4) of the variable A (cross-sectional area of the specimen in the plane of the loop) which is a function of the reinforcing bar diameter. The scatter is probably due to random variation of the con-
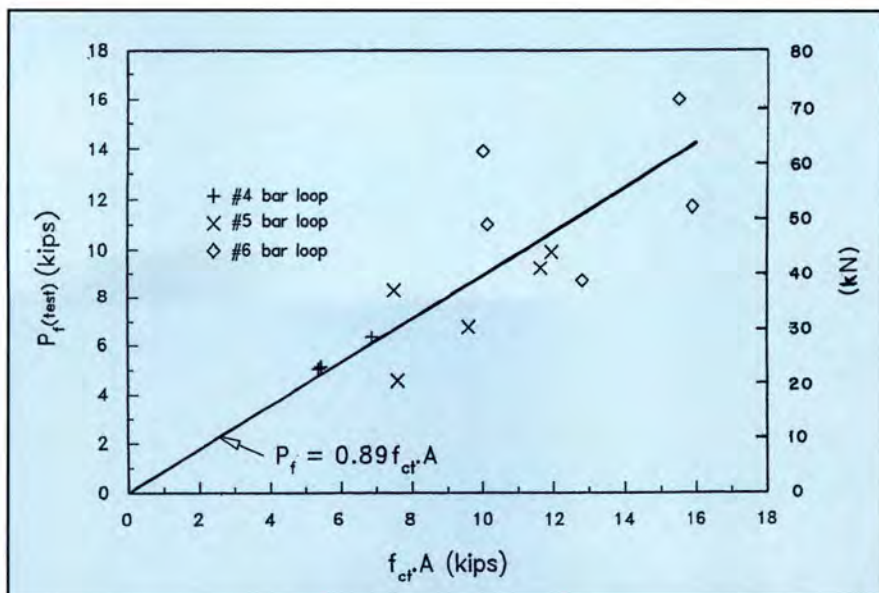

Fig. 8. Variation of P_f with the tensile strength of the plane containing the loop $f_{ct}A$, when lateral force F_n is zero.
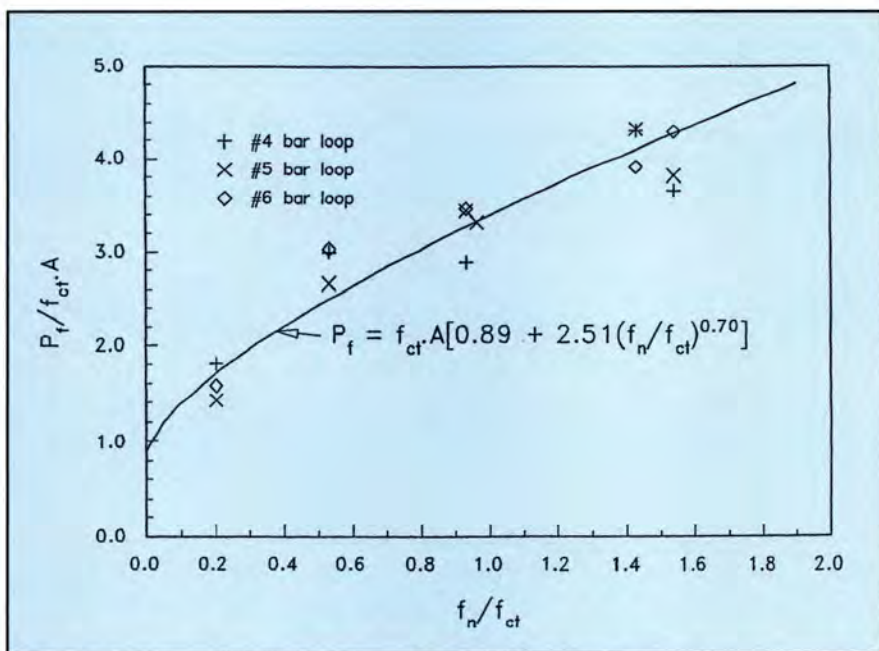

Fig. 9. Series B — Specimens with concentric lateral force ($e^* = 0$).

crete tensile strength and to the influence of any small misalignment of the reinforcing bar relative to the bearing face of the specimen.

Eq. (2), derived from the CEB-FIP Model Code Eq. (17.8), was also used to calculate the anchorage strength of the specimens of Series A. Using this equation, the average value of the ratio $P_f(\text{test})/P_f(\text{calc.})$ for Series A is 1.12 with a standard deviation of 0.45, i.e., not as satisfactory as using Eq. (4).

Series B, concentric lateral force — Because the failure mode of the

specimens of this test series was also splitting of the concrete in the plane of the loop, it appeared that the pull-out strength would probably depend on the tensile strength of the specimen in the plane of the loop, $f_{ct}A$, and also on the magnitude of the uniform compressive stress, f_n, acting in the plane of the loop.

It was found that the best correlation was obtained when $P_f/(f_{ct}A)$ was plotted against (f_n/f_{ct}), as in Fig. 9; the scatter of the data is less than in the case of Series A. This is probably due
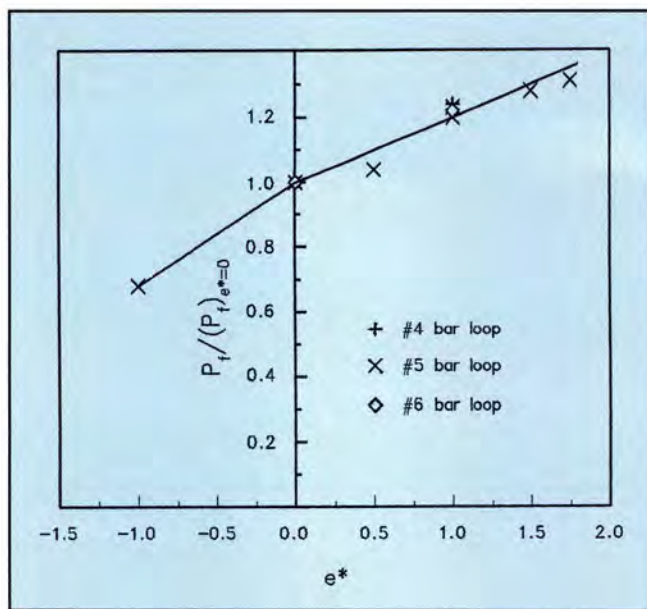
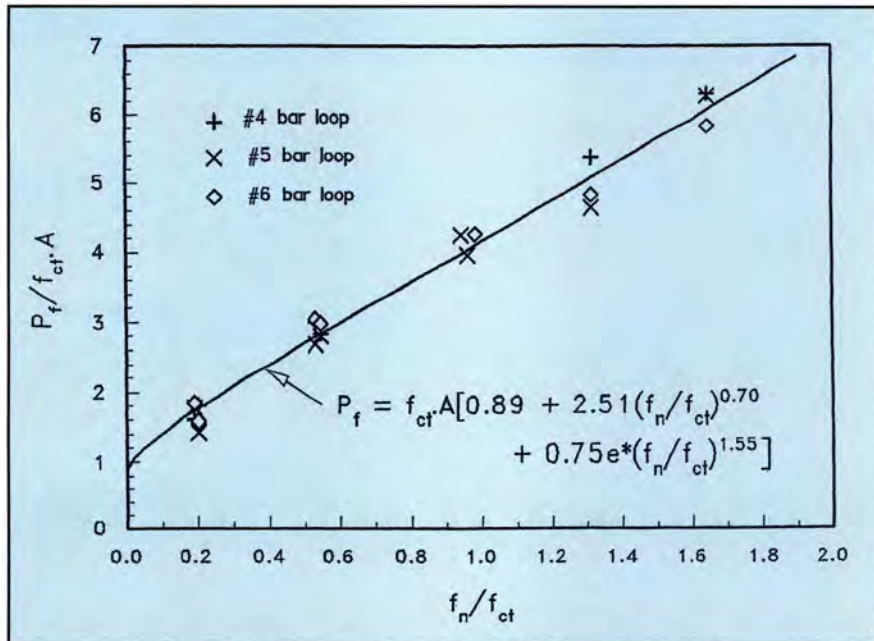Fig. 10. Variation of pull-out strength with eccentricity of lateral force.

Fig. 11. Series C — Specimens with eccentric lateral force ($e^* = 1.0$).

to the fact that, to cause a splitting failure, the pull-out force must overcome the compressive stress in the plane of the loop in addition to the tensile strength of the concrete. Hence, the influence of random variations in the concrete tensile strength will have less effect on the failure load. The best fit line to the experimental data is given by the following equation:

$$P_f = f_{ct}A[0.89 + 2.51(f_n/f_{ct})^{0.70}] \quad (5)$$

The values of P_f calculated using Eq. (5) are listed in Table 5. The aver-

age value of the ratio $P_f(\text{test})/P_f(\text{calc.})$ for Series B is 1.00, with a standard deviation of 0.111.

Series C, eccentric lateral force — When the lateral force is eccentric, the eccentricity being toward the bearing face of the specimen, the compressive stress in the plane of the loop adjacent to the bearing face is increased. This should delay the onset of cracking in the plane of the loop and may increase the resistance to a splitting failure. However, such an eccentricity of the lateral force will also cause a tensile stress near

the back face of the specimen, which could reduce any gain in splitting strength due to the higher compressive stress near the bearing face.

In Fig. 10, the pull-out strengths of loops of various sizes are plotted against the non-dimensionalized eccentricity of the lateral force. The pull-out strengths are expressed as a proportion of the pull-out strength of similar specimens subject to concentric lateral forces of the same magnitude. [The non-dimensionalized eccentricity, $e^* = e/(0.5d_b + 0.375)$, when e and d_b are in inches, $\{e^* = e/(0.5d_b + 9.53)$ when e and d_b are in mm}]. As shown in Fig. 2, e^* is considered positive when measured toward the bearing face.

It can be seen in Fig. 10 that the increase in pull-out strength is essentially proportional to the eccentricity e^*, when e^* is positive. The pull-out strength decreases at a greater rate when e^* is negative, i.e., when the eccentricity results in a tension stress on the plane of the loop adjacent to the bearing face. For simplicity, it was decided to consider that the pull-out strength increases in proportion to e^*.

In Fig. 11, $P_f/(f_{ct}A)$ has been plotted against f_n/f_{ct} for the specimens of Series C having an eccentricity e^* of 1.0. It can be seen that the scatter of the data points is further decreased, compared with the data for the specimens of Series B subjected to concentric lateral force, i.e., having $e^* = 0$. This is probably due to the increase in the compressive stress in the plane of the loop, adjacent to the bearing face, for a given magnitude of lateral force. The best fit line to the data is given by the equation:

$$P_f = f_{ct}A[0.89 + 2.51(f_n/f_{ct})^{0.70} + 0.75e^*(f_n/f_{ct})^{1.55}] \quad (6)$$

The values of P_f calculated using Eq. (6) are listed in Table 6. The average value of the ratio $P_f(\text{test})/P_f(\text{calc.})$ for the specimens of Series C with positive eccentricity of the lateral force is 1.00, with a standard deviation of 0.048. It should be noted that Eq. (5) embodies Eq. (4), and that Eq. (6) embodies both Eqs. (4) and (5).

The lower part of Fig. 11 in Ref. 5 shows the distribution of the ratio (test strength)/(calculated strength) for the

Fig. 12. Comparison of distribution of (test strength)/(calculated strength) for loop anchorages and for standard hooks.[5]

tests used to validate the provisions of Section 12.5 of ACI 318-89[3] for the development of standard hooks in tension. This data is reproduced in slightly different form in Fig. 12, together with the distribution of the results of the tests on loops reported here, using Eq. (5) to calculate the strength. It can be seen that the distribution of the ratio (test strength)/(calculated strength) for the loop tests is a little more favorable than for the case of the standard hook.

The calculated strengths of the standard hook in Ref. 5 correspond to 1.25 times the strengths given by the expression in Section 12.5.2 of ACI 318-89[3]; i.e., the provisions of Section 12.5 correspond to development of a nominal anchorage strength of 1.25 times the yield strength of the reinforcing bar, and an implicit ϕ factor of 0.8 because no explicit ϕ factor is used in design with the expression of Section 12.5.2. This same approach will be followed in developing proposals for the design of loop anchorages.

The behavior of the loop anchorage

specimens reported here is consistent with the behavior of loop anchorages in the dapped end beams reported in Ref. 2. In that case, the confining force across the loop anchorage was provided by the internal strut forces developed in the nib of the dapped end. The tests reported here demonstrated that, with adequate confining force across the loop, the loop anchorage alone is able to develop the yield strength of the reinforcing bar without an additional "lead in" length of straight bar. This was not evident from the dapped end beam tests of Ref. 2.

The present tests have also shown that loop anchorages can be used in bars of sizes Nos. 5 and 6 (16 and 19 mm in diameter), in addition to the bars of size No. 4 (13 mm in diameter) used in the dapped end beams of Ref. 3. No information has been developed as to how the anchorage provided by a loop can be increased by additional straight lengths of bar when lateral confinement is insufficient to enable the loop to develop the bar yield strength when acting alone.

CONCLUSION

Based on the test results reported above, a 180-degree loop anchorage of $6d_b$ bend diameter and with $^3/_4$ in. (19 mm) cover at the sides and at the head of the loop can develop the yield strength of reinforcing bars of sizes Nos. 4, 5, and 6 (13, 16, and 19 mm in diameter) when provided with an appropriate confining force across the plane of the loop.

PROPOSALS FOR THE DESIGN OF LOOP ANCHORAGES

To be consistent with the treatment of standard hooks in Section 12.5 of ACI 318-89[3], these proposals will ensure that the nominal pull-out strength P_n of a loop anchorage is equal to 1.25 times the yield strength of the bars leading into the loop, i.e., $P_n = 1.25A_{sl}f_y$, where A_{sl} is twice the cross section of the bar used to form the loop.

The design proposals apply to 180-degree loops of bend diameter $6d_b$ in sizes 4, 5, and 6 (13, 16, and 19 mm diameter) reinforcing bars with a minimum cover of $^3/_4$ in. (19 mm). To be conservative, the proposals will be based on Eq. (5), which relates to the case of a uniform normal stress acting on the plane of the loop. Hence, the required nominal pull-out strength is:

$$P_n = 1.25A_{sl}f_y$$
$$= f_{ct}A[0.89 + 2.51(f_n/f_{ct})^{0.70}] \quad (7)$$

This equation may be transposed to read:

$$\frac{f_n}{f_{ct}} = \left[\frac{(1.25A_{sl}f_y)/(f_{ct}A) - 0.89}{2.51}\right]^{1.429} \quad (8)$$

or, the required lateral force:

$$F_n = f_n A$$
$$= f_{ct}A\left[\frac{(1.25A_{sl}f_y)/(f_{ct}A) - 0.89}{2.51}\right]^{1.429} \quad (9)$$

Table 7 lists the values of the lateral normal force F_n required to give a nominal anchorage strength of $1.25A_{sl}f_y$ for
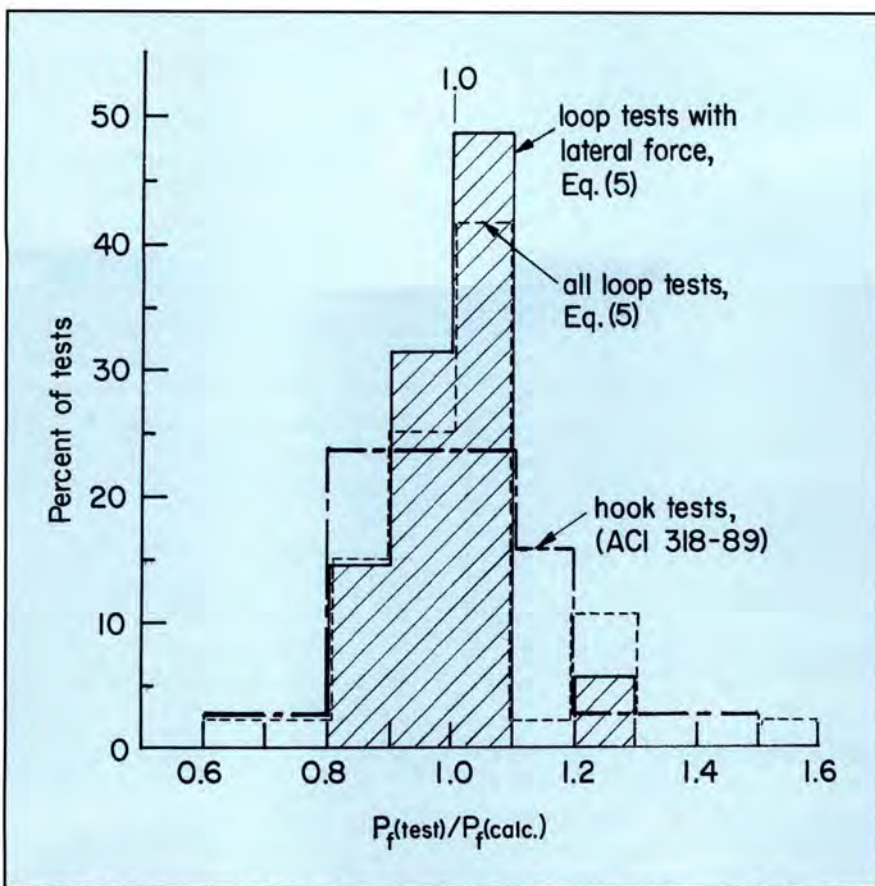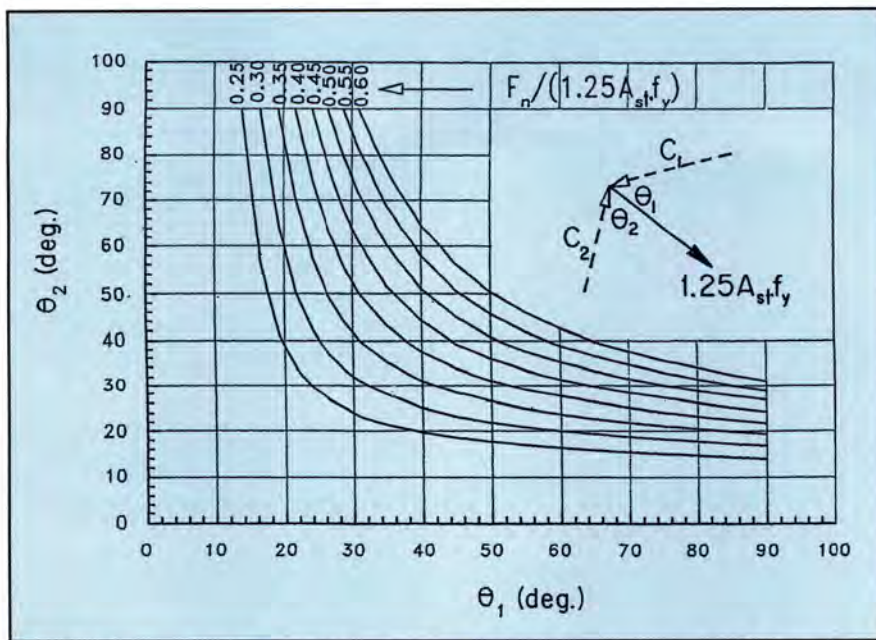
Fig. 13. Minimum value of angle θ_2 for a given angle θ_1, if P_n is equal to $1.25A_{sl}f_y$.

a looped reinforcing bar of yield strength 60 ksi (414 MPa) embedded in normal weight concrete. Also given are values of the ratio of the required normal force F_n to the required nominal anchorage strength of $1.25A_{sl}f_y$. These values were calculated using Eq. (9). A conservative value for the splitting tensile strength of normal weight concrete of $6\sqrt{f_c'}$ psi ($0.5\sqrt{f_c'}$ MPa) was used in these calculations. (This is the average value measured over a number of years for concrete made from glacial outwash gravel in Western Washington State.)

Similar calculations were made for the case of loop anchorages embedded in sand-lightweight and all-lightweight concretes, for concrete compressive strengths of 3000 and 6000 psi (21 and 42 MPa). In these cases, the splitting tensile strength was assumed to be 0.85 and 0.75 of the splitting tensile strength of the normal weight concrete for sand-lightweight and all-lightweight concretes, respectively. The values obtained are listed in Table A1 in the Appendix.

The value of the ratio of Req. F_n for sand-lightweight concrete to that required for normal weight concrete varied only between 1.11 and 1.13. Similarly, the value of the ratio of Req. F_n for all-lightweight concrete to that required for normal weight concrete varied only between 1.19 and 1.24. It is therefore proposed that, for

sand-lightweight and all lightweight concretes, the values of F_n and $F_n/(1.25A_{sl}f_y)$ listed in Table 7 be multiplied by 1.12 and 1.22, respectively.

The tabulated required values of F_n can be used to check the adequacy of a loop anchor acted on directly by a force normal to the plane of the loop, such as a beam reaction. In this case, the reaction acting on the loop anchorage cannot be less than the tabulated value of F_n.

The required ratios of F_n to $1.25A_{sl}f_y$ can be used to check the adequacy of a loop anchor when acted upon by two strut forces, C_1 and C_2, inclined at angles θ_1 and θ_2 to the plane of the loop, as shown in Fig. 13. Such a situation occurs in a dapped end at the top of inclined hanger reinforcement, as in Fig. 1. In such a case, for equilibrium:

$$C_1\cos\theta_1 + C_2\cos\theta_2 = 1.25A_{sl}f_y$$

and

$$F_n = C_1\sin\theta_1 = C_2\sin\theta_2$$

Hence,

$$C_1(\cos\theta_1 + \sin\theta_1 \times \cot\theta_2) = 1.25A_{sl}f_y$$

Thus,

$$C_1\sin\theta_1(\cot\theta_1 + \cot\theta_2) = 1.25A_{sl}f_y$$

Therefore,

$$F_n = C_1\sin\theta_1$$
$$= (1.25A_{sl}f_y)/(\cot\theta_1 + \cot\theta_2)$$

and

$$\theta_2 = \cot^{-1}[(1.25A_{sl}f_y/F_n) - \cot\theta_1]$$
(10)

Eq. (10) yields the minimum value of angle θ_2 for a given angle θ_1, if the nominal loop anchor strength is not to be less than $1.25A_{sl}f_y$. Fig. 13 shows plotted curves relating θ_1 to θ_2 according to Eq. (10) for various values of $F_n/(1.25A_{sl}f_y)$. These curves can be used in conjunction with the required values of $F_n/(1.25A_{sl}f_y)$ listed in Table 7 to check the adequacy of a loop anchorage acted on by two concrete strut forces.

The required values of F_n and $F_n/(1.25A_{sl}f_y)$ for loops made of 60 ksi (414 MPa), Nos. 4, 5, and 6 reinforcing bars, which are embedded in normal weight concrete, can be approximated quite closely by the following equations:

$$(\text{Req. } F_n)_{60}$$
$$= A_{sl}f_y(0.58 + 0.25d_b - 0.043f_c')$$
$$= 60A_{sl}(0.58 + 0.25d_b - 0.043f_c')$$
(11a)

and

$$[F_n/(1.25A_{sl}f_y)]_{60}$$
$$= (0.46 + 0.20d_b - 0.034f_c')$$
(12a)

where d_b = reinforcing bar diameter in inches; A_{sl} is in in.² and f_y and f_c' are in ksi.

Or, in SI units:

$$(\text{Req. } F_n)_{414}$$
$$= 414f_y(0.58 + 0.0098d_b - 0.0062f_c')$$
(11b)

and

$$[F_n/(1.25A_{sl}f_y)]_{414}$$
$$= (0.46 + 0.0079d_b - 0.0049f_c')$$
(12b)

where d_b is in mm, A_{sl} is in mm² and f_y and f_c' are in MPa.

Using these equations, the average ratio of (value listed in Table 7)/[value given by Eq. (11) or (12) as appropriate] is 1.00 for all listed values of F_n and $F_n/(1.25A_{sl}f_y)$, with a standard deviation of 0.013. (For the case of looped reinforcing bars embedded in sand-lightweight and all-lightweight concretes, the values given by Eqs. (11) and (12) should be multiplied by

Table 7. Required values of F_n and $[F_n/(1.25A_{sl}f_y)]$ for loop anchorages embedded in normal weight concrete, to make $P_n = 1.25 A_{sl}f_y$ when $f_y = 60$ ksi (414 MPa).

Type of loop	f_c'(psi)	3000	4000	5000	6000
No. 4 bar loop	F_n (kips)	13.86	12.53	11.54	10.74
	$F_n/(1.25A_{sl}f_y)$	0.462	0.416	0.385	0.358
No. 5 bar loop	F_n (kips)	23.03	20.92	19.34	18.07
	$F_n/(1.25A_{sl}f_y)$	0.495	0.450	0.416	0.389
No. 6 bar loop	F_n (kips)	34.04	31.00	28.72	26.90
	$F_n/(1.25A_{sl}f_y)$	0.516	0.470	0.435	0.408

Note: 1000 psi = 6.895 MPa; 1 kip = 4.46 kN.

For loop anchorages embedded in sand-lightweight and all-lightweight concretes, the values in Table 7 should be multiplied by 1.12 and 1.22, respectively.

1.12 and 1.22, respectively.)

The values of F_n and $F_n/(1.25A_{sl}f_y)$ listed in Table 7 and those given by Eqs. (11) and (12) are only valid for loop anchorages in reinforcing bars with a yield strength of 60 ksi (414 MPa). To extend the usefulness of these proposals, a parametric study was made of the relationship between the values of F_n and $F_n/(1.25A_{sl}f_y)$ required when $f_y = 60$ ksi (414 MPa), to those required when $f_y = 40$, 50, and 75 ksi (276, 345, and 517 MPa), calculated using Eq. (9). It was found that for f_y in this range, the required values of F_n and of $F_n/(1.25A_{sl}f_y)$ are approximated very closely by the following relationships:

$$\text{Req. } F_n = (\text{Req } F_n)_{60}(f_y/60)^{1.76}$$
(13a)

and

$$\text{Req. } F_n/(1.25A_{sl}f_y)$$
$$= [\text{Req. } F_n/(1.25A_{sl}f_y)]_{60}[(f_y/60)^{0.76}]$$
(14a)

or in SI units:

$$\text{Req. } F_n = (\text{Req } F_n)_{414}(f_y/414)^{1.76}$$
(13b)

and

$$\text{Req. } F_n/(1.25A_{sl}f_y)$$
$$= [\text{Req. } F_n/(1.25A_{sl}f_y)]_{414}[(f_y/414)^{0.76}]$$
(14b)

When applied to all combinations of bar sizes 4, 5, and 6 (13, 16, and 19 mm in diameter), bar yield strengths of 40, 50, 60, and 75 ksi (276, 345, 414, and 517 MPa) and concrete strengths f_c' of 3000, 4000, 5000, and 6000 psi (21, 28, 35, and 42 MPa), the average of [value calculated using Eq. (9)]/[value calculated using Eq. (13) or (14) as appropriate] was 0.993, with a standard deviation

of 0.017. Numerical values are listed in Tables A2 and A3 in the Appendix.

DESIGN PROPOSALS FOR LOOP ANCHORAGES

This section summarizes design proposals for 180-degree loop anchorages with bend diameter $6d_b$ for Nos. 4, 5, and 6 reinforcing bars.

The adequacy of a loop anchorage may be checked using either of the following methods:

1. Check that the lateral force acting normal to the plane of the loop at factored load is not less than the value of F_n given in Table 7 [or by Eq. (11)], multiplied by $(f_y/60)^{1.76}$ if using customary units, or by $(f_y/414)^{1.76}$ if using SI units. Note: In the case of loop anchorages embedded in sand-lightweight and all-lightweight concretes, the values of F_n listed in Table 7 [or calculated using Eq.(11)], should be multiplied by 1.12 and 1.22, respectively.

2. Using the curves in Fig. 13, check that the relationship of the angles θ_1 and θ_2 between the compression struts C_1 and C_2 meeting at the loop anchorage and the plane containing the loop is satisfactory. The value of $F_n/(1.25A_{sl}f_y)$ used to enter the curves in Fig. 13 is the required $F_n/(1.25A_{sl}f_y)$ given by Table 7 [or by Eq. (12)], multiplied by $(f_y/60)^{0.76}$ if using customary units, or by $(f_y/414)^{0.76}$ if using SI units. Note: In the case of loop anchorages embedded in sand-lightweight and all-lightweight concretes, the values of $F_n/(1.25A_{sl}f_y)$ listed in Table 7 [or calculated using Eq. (12)], should be multiplied by 1.12 and 1.22, respectively.

DESIGN EXAMPLES

Example 1

Check the anchorage of the looped No. 4 (12.7 mm diameter) reinforcing bar, $f_y = 60$ ksi (414 MPa), that is serving as the hanger reinforcement in the dapped end double tee beam shown in Fig. 14. This is the design example for this type of reinforcement scheme, set out in Appendix E of Ref. 2. The beam is made of normal weight concrete, for which $f_c' = 5000$ psi (34.5 MPa).

The reinforcement in this dapped end was designed as proposed in Section (d) of Appendix D of Ref. 2. Forces C_1 and C_2 are assumed to pass through the centroid of the reinforcing bar loop, which is located a distance $2.5d_b$ from the outside of the head of the loop. Cover of $^3/_4$ in. (19.1 mm) is provided above the head of the loop.

The inclined force C_1 has a vertical component equal to the shear V_{cr}, given by:

$$V_{cr} = 2b_d d_d \sqrt{f_c'} \text{ lb}$$

or

$$V_{cr} = (b_d d_d/6) \sqrt{f_c'} \text{ N}$$
[ACI 318 Eq. (11-3)][3]

and a horizontal component $C_1\cos\gamma_1$, determined by considering horizontal equilibrium across a vertical plane through the re-entrant corner of the dap. Angle γ_1 is then given by:

$$\gamma_1 = \tan^{-1}[V_{cr}/(C_1\cos\gamma_1)]$$

and

$$\theta_1 = 60 + \gamma_1$$

For purposes of checking the adequacy of the loop anchorage, it is conservative to consider force C_2 as acting between the centroid of the loop and the point of intersection of the center line of the nib flexural reinforcement and the centerline of the vertical reaction.

Hence, $\gamma_1 = 15.7$ degrees and $\theta_1 = 75.7$ degrees, and $\gamma_2 = 21.0$ degrees and $\theta_2 = 51.0$ degrees.

For a No. 4 bar loop in 60 grade reinforcing bar embedded in 5000 psi (34.5 MPa) normal weight concrete, using Table 7:
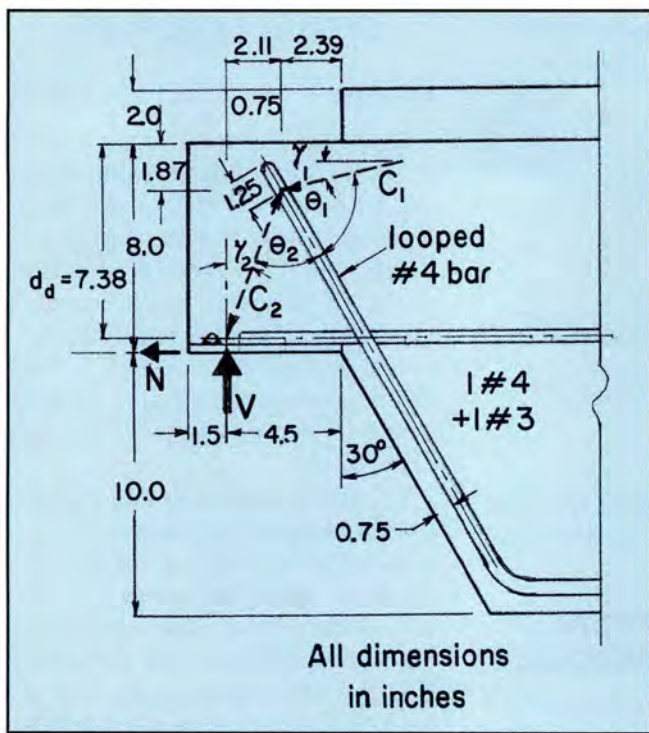
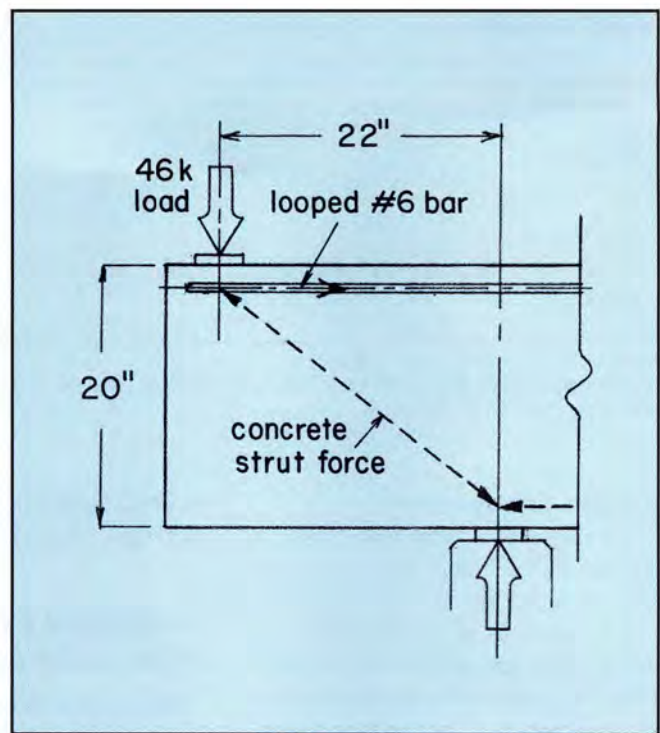Fig. 14. Example 1 — Anchorage of looped hanger reinforcement.

Fig. 15. Example 2 — Reinforcement at end of precast concrete beam.

Req. $F_n/(1.25A_{sl}f_y) = 0.385$

Then from Fig. 13, minimum value of θ_2 when $\theta_1 = 75.7$ degrees is 24 degrees, which is less than 51 degrees.

Therefore, anchorage of looped No. 4 (12.7 mm) bar is satisfactory.

Note: $[F_n/(1.25A_{sl}f_y)]_{60}$ could have alternatively been calculated using:

$$[F_n/(1.25A_{sl}f_y)]_{60}$$
$$= (0.46 + 0.20d_b - 0.034f'_c) \qquad (12a)$$

Substituting values in Eq. (12a):

$$[F_n/(1.25A_{sl}f_y)]_{60}$$
$$= [0.46 + 0.20(0.5) - 0.034(5)]$$
$$= 0.390$$

This value is 1.3 percent above the value listed in Table 7.

Example 2

A 20 in. (508 mm) deep precast concrete beam projects 26 in. (660 mm) beyond its support, and carries a factored concentrated load of 46 kips (205 kN) 4 in. (102 mm) from its end (see Fig. 15). The negative flexural reinforcement consists of a No. 6 (19.1 mm diameter) reinforcing bar looped in the horizontal plane at the end of the beam [$f_y = 75$ ksi (517 MPa)]. Because the beam depth is large in relation to the distance from the load to the support, this flexural reinforcement must develop its yield strength at the location of the concentrated load. Check the adequacy of the loop anchorage, if the concrete is normal weight concrete with $f'_c = 5000$ psi (34.5 MPa).

Req. $F_n = (F_n)_{60}(f_y/60)^{1.76}$

From Table 7, $(F_n)_{60} = 28.72$ kips

Therefore, Req. $F_n = (28.72)(75/60)^{1.76}$
$$= 42.53 \text{ kips}$$

This value is less than the concentrated load and, therefore, the anchorage should be adequate.

Note: $(F_n)_{60}$ could alternatively have been calculated using:

$$(\text{Req. } F_n)_{60}$$
$$= A_{sl}f_y(0.58 + 0.25d_b - 0.043f'_c)$$
$$= 60A_{sl}(0.58 + 0.25d_b - 0.043f'_c) \qquad (11a)$$

Substituting values in Eq. (11a):

$$(\text{Req. } F_n)_{60} = 60(0.88)[0.58 + 0.25(0.75) - 0.043(5)]$$
$$= 29.17 \text{ kips } (129.7 \text{ kN})$$

This force is 1.02 times the value obtained from Table 7.

REFERENCES

1. Schlaich, J., Schafer, K., and Jennewein, M., "Toward a Consistent Design of Structural Concrete," PCI JOURNAL, V. 32, No. 3, May-June 1987, pp. 74-150.
2. Mattock, A. H., and Theryo, T. S., "Strength of Members With Dapped Ends," Final Report, PCISFRAD Project No. 6, Precast/Prestressed Concrete Institute, Chicago, IL, 1986.
3. ACI Committee 318, "Building Code Requirements for Reinforced Concrete, (ACI 318-89)," American Concrete Institute, Detroit, MI, 1989.
4. CEB-FIP Model Code for Concrete Structures, Comité Euro-International du Béton (CEB), London, 1978.
5. Jirsa, J. O., Lutz, L. A., and Gergely, P., "Rationale for Suggested Development, Splice, and Standard Hook Provisions for Deformed Bars in Tension," Concrete International, V. 1, No. 7, July 1979, pp. 47-61.

APPENDIX A

Table A1. Effect of type of concrete on required values of F_n (kips).

Type of concrete	f_c'(psi)	No. 4 bar loop	No. 5 bar loop	No. 6 bar loop
Normal weight	3000	13.86	23.03	34.04
Sand-lightweight		15.41	25.51	37.62
Ratio		1.11	1.11	1.11
All-lightweight		16.66	27.49	40.49
Ratio		1.20	1.19	1.19
Normal	6000	10.74	18.07	26.90
Sand-lightweight		12.17	20.35	30.17
Ratio		1.13	1.13	1.12
All-lightweight		13.31	22.16	32.78
Ratio		1.24	1.23	1.22

Note: 1000 psi = 6.895 MPa; 1 kip = 4.46 kN.

Table A2. Effect of variation of reinforcement yield strength on required F_n (kips).

f_c'(psi)	3000	4000	5000	6000
f_y = 40 ksi				
(F_n) No. 4	6.83	6.02	5.41	4.92
Approximate (F_n) No. 4*	6.79	6.14	5.65	5.26
Ratio†	1.01	0.98	0.96	0.94
(F_n) No. 5	11.51	10.23	9.27	8.49
Approximate (F_n) No. 5*	11.28	10.25	9.47	8.85
Ratio†	1.02	1.00	0.98	0.96
(F_n) No. 6	17.15	15.31	13.92	12.82
Approximate (F_n) No. 6*	16.68	15.19	14.07	13.18
Ratio†	1.03	1.01	0.99	0.97
f_y = 50 ksi				
(F_n) No. 4	10.16	9.10	8.30	7.66
Approximate (F_n) No. 4*	10.06	9.09	8.37	7.79
Ratio†	1.01	1.00	0.99	0.98
(F_n) No. 5	16.97	15.29	14.02	13.01
Approximate (F_n) No. 5*	16.71	15.18	14.03	13.11
Ratio†	1.02	1.01	1.00	0.99
(F_n) No. 6	25.17	22.75	20.92	19.47
Approximate (F_n) No. 6*	24.70	22.49	20.84	19.52
Ratio†	1.02	1.01	1.00	1.00
f_y = 75 ksi				
(F_n) No. 4	20.02	18.27	16.95	15.90
Approximate (F_n) No. 4*	20.53	18.56	17.09	15.91
Ratio†	0.98	0.99	0.99	1.00
(F_n) No. 5	33.07	30.28	28.18	26.52
Approximate (F_n) No. 5*	34.11	30.98	28.64	26.76
Ratio†	0.97	0.98	0.98	0.99
(F_n) No. 6	48.74	44.70	41.68	39.28
Approximate (F_n) No. 6*	50.41	45.91	42.53	39.84
Ratio†	0.97	0.97	0.98	0.99

Note: 1 ksi = 1000 psi = 6.895 MPa; 1 kip = 4.46 kN.

* Approximate $F_n = (F_n)_{60} (f_y/60)^{1.76}$ where $(F_n)_{60}$ is value of (F_n) when f_y = 60 ksi.
  In SI units, Approximate $F_n = (F_n)_{414} (f_y/414)^{176}$ where $(F_n)_{414}$ is value of (F_n) when f_y = 414 MPa.
† Ratio = (F_n)/[Approximate (F_n)].

Table A3. Effect of variation of reinforcement yield strength on required $[F_n/(1.25A_{sl}f_y)]$.

f'_c(psi)	3000	4000	5000	6000
f_y = 40 ksi				
Q No. 4*	0.341	0.301	0.270	0.246
Approximate Q No.4†	0.339	0.306	0.283	0.263
Ratio‡	1.01	0.98	0.96	0.94
Q No. 5*	0.371	0.330	0.299	0.274
Approximate Q No. 5†	0.364	0.331	0.306	0.286
Ratio‡	1.02	1.00	0.98	0.96
Q No. 6*	0.390	0.348	0.317	0.291
Approximate Q No. 6†	0.379	0.345	0.320	0.300
Ratio‡	1.03	1.01	0.99	0.97
f_y = 50 ksi				
Q No. 4*	0.406	0.364	0.332	0.306
Approximate Q No. 4†	0.402	0.362	0.335	0.312
Ratio‡	1.01	1.00	0.99	0.98
Q No. 5*	0.438	0.394	0.362	0.336
Approximate Q No. 5†	0.431	0.392	0.362	0.339
Ratio‡	1.02	1.00	1.00	0.99
Q No. 6*	0.458	0.414	0.380	0.354
Approximate Q No. 6†	0.449	0.409	0.379	0.355
Ratio‡	1.02	1.01	1.00	1.00
f_y = 75 ksi				
Q No. 4*	0.534	0.487	0.452	0.424
Approximate Q No. 4†	0.547	0.493	0.456	0.424
Ratio‡	0.98	0.99	0.99	1.00
Q No. 5*	0.569	0.521	0.485	0.456
Approximate Q No. 5†	0.586	0.533	0.493	0.461
Ratio‡	0.97	0.98	0.98	0.99
Q No. 6*	0.591	0.542	0.505	0.476
Approximate Q No. 6†	0.611	0.557	0.515	0.483
Ratio‡	0.97	0.97	0.98	0.99

Note: 1 ksi = 1000 psi = 6.895 MPa; 1 kip = 4.46 kN.

* $Q = [F_n/(1.25 A_{sl}f_y)]$

† Approximate $Q = Q_{60} (f_y/60)^{0.76}$, where Q_{60} is the value of $[F_n/(1.25 A_{sl}f_y)]$ when f_y = 60 ksi.
In SI units, Approximate $Q = Q_{414} (f_y/414)^{0.76}$, where Q_{414} is the value of $[F_n/(1.25 A_{sl}f_y)]$ when f_y = 414 MPa.

‡ Ratio = Q/(Approximate Q) = $[F_n/(1.25 A_{sl}f_y)]$/{Approximate $[F_n/(1.25 A_{sl}f_y)]$}.

APPENDIX B — NOTATION

A = cross-sectional area of specimen in the plane of the loop, in.^{2} (mm^2)

A_{sl} = cross-sectional area of reinforcing bars leading into loop, i.e., twice the cross-sectional area of the bar used to form the loop, in.^{2} (mm^2)

c = side cover to loop, in. (mm)

C = concrete strut compression force, kips (kN)

d_b = reinforcing bar diameter, in. (mm)

D = reinforcing bar bend diameter, in. (mm)

e = eccentricity to lateral force with respect to centroid of specimen cross section, in. (mm)

$e*$ = non-dimensionalized eccentricity,
= $e/(0.5d_b + 0.375)$, d_b in in.
= $e/(0.5 d_b + 9.53)$, d_b in mm

f'_c = concrete compressive strength measured on 6 x 12 in. (150 x 300 mm) cylinders, psi or ksi (MPa)

f_{cd} = CEB design concrete compressive strength (MPa)

f_{ck} = CEB concrete characteristic strength, MPa = $(f_{cm} - 8$ MPa)

f_{cm} = CEB concrete mean compressive strength, measured on 150 x 300 mm cylinders, MPa

f_{ct} = concrete splitting tensile strength measured on 6 x 12 in. (150 x 300 mm) cylinders, psi or ksi (MPa)

f_n = lateral (normal) stress acting on the concrete in the plane of the loop, psi or ksi (MPa)

f_s = stress in reinforcing bar at start of bend, psi (MPa)

f_y = reinforcing bar yield stress, ksi (MPa)

F_n = lateral force applied to specimen, normal to the plane of the loop, kips (kN)

P_f = pull-out load in loop anchor tests, kips (kN)

P_n = nominal pull-out strength of loop anchor in design, kips (kN)

γ_c = CEB concrete strength reduction factor = 1.5

θ = angle between concrete strut force and plane of loop anchorage